THE JOURNAL OF PHYSICAL CHEMISTRY A

Article

pubs.acs.org/JPCA

Cooling by H_3^+ Emission

Steve Miller,*[,†] Tom Stallard,[‡] Jonathan Tennyson,[†] and Henrik Melin[‡]

[†]Department of Physics and Astronomy, University College London, London WC1E 6BT, U.K.

[‡]Department of Physics and Astronomy, University of Leicester, University Road, Leicester LE17RH, U.K.

ABSTRACT: Emission by the H_3^+ molecular ion may be important in determining the energy balance in astrophysical situations, such as in (exo)planetary atmospheres. Here we report the calculation of a new cooling function, based on refitted partition functions and a recalculation of the total energy emitted by the molecule. This new function gives significantly increased cooling at higher temperatures, typical of those found in the atmospheres of gas giants. It is shown that nonthermal effects also need to be considered. A link to a web-based code to calculate radiative cooling in H_2/H_3^+ gas mixtures, including the effects of departures from equilibrium, is provided.

INTRODUCTION

The existence of a species with a mass-to-charge ratio of 3 was first reported by J. J. Thomson[1] in 1911, which he originally labeled X_3. At lectures at the Royal Institution[2] and Royal Society,[3] Thomson publicly identified X_3 as a "new" form of hydrogen, H_3^+. Generally speaking, the spectrum of a candidate new molecule is needed to confirm any new discovery. In this case of H_3^+, seven decades were to pass before Oka[4] finally claimed that prize in 1980, measuring fifteen infrared lines in a wavelength region of 500 cm^{-1} centered on 2700 cm^{-1} (3.704 μm). The reason it took so long and the far-reaching consequences of Oka's measurements will be outlined below.

"New" is, of course, a relative term. The honor of being the first molecule formed in the Universe goes to HeH^+: because the ionization potential of He (24.6 eV) is considerably higher than that of H (13.6 eV), neutral He forms earlier after the Big Bang, during the early part of the Recombination Era, and can combine with H^+ (with no activation energy required). Some time prior to 10 million years after the Big Bang, the following chemical pathways became available:[5,6]

$$\begin{aligned} H + H^+ &\rightarrow H_2^+ + h\nu \\ H_2^+ + H &\rightarrow H_2 + H^+ \\ H_2 + H^+ &\rightarrow H_3^+ + h\nu \\ H_2^+ + H_2 &\rightarrow H_3^+ + H \end{aligned} \quad (1)$$

(The last of this series of reactions was first described in 1925 by Hogness and Lunn[7] and was the key reaction to forming H_3^+ in the interstellar medium and planetary atmospheres.) As a result, H_3^+ is the sixth most abundant of 11 early universe molecules listed by Glover and Savin,[8] with a peak abundance relative to the total gas number density of a few 10^{-12}. This peak abundance occurs in clouds collapsing to form a Population III star, at a point that the gas density reaches some 10^{14} m^{-3}. So though a newcomer relative to HeH^+, H_3^+ still goes back a long way: Thomson's "new" form of hydrogen was new to human knowledge, but very old in astronomical terms.

Star formation from proto-stellar nebulae requires cooling, and in the early universe—before the first generation of stars can enrich the gas with elements heavier than lithium—that is predominantly supplied by radiation from H_2. The absence of a permanent dipole, or one induced when the molecule vibrates, means that H_2 is, per molecule, a very poor radiator: it relies on quadrupole emission,[9] which typically results in very small Einstein A coefficients for spontaneous emission (A_{if}) of 10^{-5} – 10^{-7} s^{-1}.

Although, according to Glover and Savin,[8] the H_3^+ abundance relative to H_2 never rises above a few 10^{-9}, at a point when the overall gas density is $\sim 10^{14}$ m^{-3} and that of H_2 itself is $\sim 10^{11}$ m^{-3}. Nonetheless, H_3^+ contributes up to 3% of the total cooling of the contracting gas cloud. With D_{3h} equilibrium geometry, H_3^+ also has no permanent dipole, but it does have one that is induced when the molecule vibrates in a manner that distorts and lowers that symmetry. Its ν_2 antisymmetric-stretch/bend mode generates ro-vibrational transitions with A_{if} typically in the range 10^1–10^2 s^{-1}, many orders of magnitude greater than those of H_2.[10] Moreover, H_3^+ is a "floppy" molecule in the terminology of Tennyson and Sutcliffe,[11] with large anharmonicities in the vibrational modes and large centrifugal forces complicating its rotational energy level structure. This also means distorted, rotating H_3^+ can exhibit a dipole-driven pure rotational spectrum.[12,13] This "forbidden" rotational spectrum has yet to be observed but is an important cooling agent, especially at lower temperatures.

The downside of this floppiness is that it made it difficult for spectroscopists to predict and interpret the spectrum: Oka[4]

Special Issue: Oka Festschrift: Celebrating 45 Years of Astrochemistry

Received: December 18, 2012
Revised: July 16, 2013
Published: July 16, 2013

   dx.doi.org/10.1021/jp312468b | J. Phys. Chem. A 2013, 117, 9770–9777

spent many days searching for lines once he had found the first transition, and it took the complicated Hamiltonian developed by Watson to assign them.[14] The upside of ease with which H_3^+ geometry departs from its equilibrium configuration is that many transitions that would be forbidden in a harmonic system (overtones, difference bands, and even symmetric-stretch transitions) have relatively large A_{if} values.[15] The result is a rich and somewhat irregular spectrum, covering a large spectral range from the orange part of the visible[16] and near-infrared,[4,17−25] through the mid-infrared, toward the microwave,[12,13] although only one transition in the mid-infrared has been claimed to have been observed,[26] and none yet in the microwave.

As one of a small group of early universe molecules, and a species that is easily formed if there is an abundance of H_2 and a source of ionization, H_3^+ has long been considered an important component of the interstellar medium, particularly in less dense environments where EUV radiation and cosmic rays can penetrate.[27,28] So it was natural that it was proposed fairly early in the history of astrochemistry as a candidate for detection,[29,30] although, typically for the history of H_3^+, it took several decades before it was first detected in an extra-solar-system source,[31] and was subsequently found where it should[32] and where it should not have been.[33−35] But the very first detection of H_3^+ outside of the laboratory really was where it was least expected—in terms of both spectroscopy and its location.

H_3^+ IN PLANETARY ATMOSPHERES

Although models of the upper atmospheres of the giant planets had predicted that H_3^+ would be a major ion there,[36,37] no one actually had proposed observations to look for it. Instead, two groups looked for quadrupole lines of H_2, which they anticipated would be detectable in emission in Jupiter's auroral/polar regions. These lines were indeed found,[38,39] but they were measured along with several other emission lines in the atmospheric K window, in the region 1.9−2.4 μm.[39] These lines were assigned as belonging to the overtone band of H_3^+ as a result of comparisons between unassigned laboratory spectra and first principles calculations of higher ro-vibrational transitions.[17]

The intensity of the overtone lines meant that planetary scientists were soon able to detect even stronger emission from the fundamental ν_2 band in the atmospheric L and L′ windows (from 2.9 to 4.2 μm).[40−42] Since the 1990s, the fundamental band has been detected in emission in Saturn[43] and Uranus,[44] along with hot bands[45] and hot overtones[46] from Jupiter. No H_3^+ emission has been detected from Neptune, however.[47] General circulation models (GCMs) of the upper atmospheres of Jupiter[48,49] and Saturn[50,51] have incorporated H_3^+ to varying degrees, as have GCMs of "hot Jupiter" exoplanets.[52]

The role of H_3^+ as a tracer of energy inputs from the magnetosphere, as a source of conductivity and heating, and as a driver of atmospheric winds, has been discussed in a number of conferences.[53−57] One key issue that has come to light is the role H_3^+ emission plays in cooling giant planet atmospheres,[51,52,58,59] a property that has been termed the "H_3^+ thermostat". Indeed, for giant exoplanets, GCMs have shown that this thermostatic effect controls the orbital radius inside of which the planet's atmosphere is no longer in hydrostatic equilibrium but starts to lose mass by hydrodynamic outflow,[52] although this is also affected by the eccentricity of the orbit.[60]

The importance of this H_3^+ thermostat has prompted us to look at the adequacy of attempts to model it and to propose some improvements. To do this, we look at the use of H_3^+ linelists and the generation of cooling functions, assuming local thermodynamical equilibrium (LTE), and attempts to parametrize those curves. We also look at the way non-LTE effects can be taken into account when gas densities fall below those critical to ensure that level populations are controlled by collisional effects, rather than radiative depopulation.

THE H_3^+ PARTITION FUNCTION

Early attempts[61,62] to calculate the partition function of H_3^+ suffered from the relatively low number of energy levels that were available, from either spectroscopic measurement or calculation. For example, the 1992 partition function of Sidhu et al.[62] only covered the first ten vibrational levels with angular momentum $J \leq 12$, based on the 1991 linelist of Kao et al.[10] In 1995, however, Neale and Tennyson[63] (henceforth NT) published explicitly calculated values for all the energy levels of H_3^+ with energies up to 15 000 cm^{-1} and an angular momentum $J \leq 20$. From this, they calculated a partition function, $z(T)$, for the molecule that was between 10 and 100 times greater above 4000 K than some previously published values.[61,62] They parametrized this with a form

$$z(T) = \sum_n a_n (\log_{10} T)^n \tag{2}$$

with $n = 0-6$. They found the best fit over the entire range of their values of $z(T)$ for H_3^+, which varied from 7.36 at 100 K, through 14 259 at 5000 K, to 57 503 at 10 000 K, was given with the values

$$a_0 = 78.6233962485680706$$
$$a_1 = -134.822002886523251$$
$$a_2 = 88.4482694968956480$$
$$a_3 = -25.9274134010262429$$
$$a_4 = 2.60233376654769222$$
$$a_5 = 0.224167420795110400$$
$$a_6 = -0.0452550693680233290$$

For 15 years, the NT partition function was the most reliable available and was used in the generation of cooling curves. This partition function also proved crucial in developing models of cool, metal-free white dwarves that were consistent with observations.[64] However, one problem with fitting to $\log_{10} T$ is that, though the errors in the log-fit may be relatively small, these can scale up to quite large errors in the actual value, which would be derived from a direct calculation that would be obtained from

$$z(T) = \sum_N g_N (2J_N + 1) \exp(-E_N/kT) \tag{3}$$

where N is the energy level number, g_N and J_N are the nuclear spin degeneracy and angular momentum of that level, respectively, and the sum is over the total number of energy levels. For this reason, Miller et al.[59] carried out a direct recalculation of $z(T)$ and then fitted to the actual value of $z(T)$ rather than the $\log_{10}$ of that value. The resultant fit was to the following form:

dx.doi.org/10.1021/jp312468b | J. Phys. Chem. A 2013, 117, 9770−9777

Table 1. Fit Coefficient for the Partition Function $z(T) = \Sigma_n A_n T^n$ for NT All Levels[59]

range	100−1800 K	1800−5000 K	5000−10000 K
A_0	−1.11391	−22125.5	−654293.0
A_1	+0.0581076	+51.1539	+617.630
A_2	+0.000302967	−0.0472256	−0.237058
A_3	-2.83724×10^{-7}	$+2.26131 \times 10^{-5}$	$+4.74466 \times 10^{-5}$
A_4	$+2.31119 \times 10^{-10}$	-5.85307×10^{-9}	-5.20566×10^{-9}
A_5	-7.15895×10^{-14}	$+7.90879 \times 10^{-13}$	$+3.05824 \times 10^{-13}$
A_6	$+1.00150 \times 10^{-17}$	-4.28349×10^{-17}	-7.45152×10^{-18}

Table 2. Fit Coefficients for the Partition Function $z_{fp}(T) = \Sigma_n A_n T^n$ Obtained Using NT First Principles Levels Only

range	100−1800 K	1800−5000 K	5000−10000 K
A_0	−1.11391	−378.621	+6200.41
A_1	+0.0581076	+0.839719	−4.55558
A_2	+0.000302967	−0.000349567	+0.000805172
A_3	-2.83724×10^{-7}	$+5.17514 \times 10^{-8}$	$+2.53004 \times 10^{-7}$
A_4	$+2.31119 \times 10^{-10}$	$+7.79447 \times 10^{-11}$	-4.69402×10^{-11}
A_5	-7.15895×10^{-14}	-1.63248×10^{-14}	$+3.06177 \times 10^{-15}$
A_6	$+1.00150 \times 10^{-17}$	$+9.60597 \times 10^{-19}$	-7.34376×10^{-20}

$$z(T) = \sum_n A_n T^n \tag{4}$$

again with n ranging from 0 to 6. For this fit, however, it was found that $z(T)$ had to be broken into a series of ranges, if a good correspondence was to be obtained. The values obtained for the coefficients are given in Table 1.

Miller et al.[59] showed that the NT fit overestimated the value of $z(T)$ for the entire temperature range they had calculated, ranging from a factor of 2.5 at 100 K to a few percent at temperatures over 5000 K. By comparison, the new fit had a maximum error of +1.7% at 3000 K and was generally well within 1% of the directly computed value.

The functions for $z(T)$ discussed above are for the value calculated from *all* the levels calculated by NT. But above J = 20 and 15 000 cm^{-1}, these were not calculated from first principles, but from Padé approximants. However, lower values of $z(T)$ were obtained if only the first principles (FP) levels were included in the summation. Miller et al.[59] thus carried out a fit for the $z_{FP}(T)$ partition function, because above 15 000 cm^{-1} there are no available Einstein A_{if} coefficients for spontaneous emission, and thus the contribution due to these higher states could not be included in any subsequent calculation of the cooling curve. This led to the parametrization given in Table 2. Again the fit to $z_{FP}(T)$ was excellent, with a maximum error of 1.2% at 100 K, and subsequent errors of 0.2−0.002% as the temperature increased.

THE H_3^+ COOLING CURVE

Neale et al.[65] (henceforth NMT) used the wave functions associated with the NT energy levels to compute a linelist of over 6.2 million transitions from which some 3.2 million were removed as they had A_{if} values that were less than 10^{-7} s^{-1}. This still left 3 070 571 individual lines with their associated wavenumbers and A_{if} values.

From this NMT calculated the per molecule emission curve, $E(H_3^+,T)$ assuming LTE. Their results showed that their linelist gave an almost complete representation up to 4000 K, a temperature above which considerable thermal dissociation would take place. They did not, however, parametrize this curve. Moreover, the overall per molecule emission was based on using the NT value of $z(T)$, which overestimates the true value: Thus any cooling curve based on the full NT partition function will underestimate the true cooling rate because $E(H_3^+,T)$ is inversely proportional to $z(T)$.

To calculate the cooling due to H_3^+ in giant planetary atmospheres, Melin[67] produced a per molecule cooling curve making use of only the transitions that fell within the wavelength range 2−5 μm, the region in which the molecule's emissions peak in the temperature range normally sampled in Jupiter. (These wavelengths correspond to the peak emission, λ_{max}, of a blackbody with T in the range 1500−600 K.) Melin[66] made use of the Neale−Tennyson fit to their full level partition function, using

$$E(H_3^+,T) = \sum_n B_n T^n \tag{5}$$

The resulting cooling curve was fitted with n = 0−4 (Table 3).

Table 3. Fit Coefficients for the Cooling Function $E(H_3^+,T) = \Sigma_n B_n T^n$ Given by Melin (2006) in Units of Watts $Molecule^{-1}$ $Sterradian^{-1}$

range	500−900 K	900−1800 K
B_0	-6.11904×10^{-21}	-8.24045×10^{-21}
B_1	$+4.96694 \times 10^{-23}$	$+3.54583 \times 10^{-23}$
B_2	-1.43608×10^{-25}	-8.66269×10^{-26}
B_3	$+1.60926 \times 10^{-28}$	$+9.76608 \times 10^{-29}$
B_4	-3.87932×10^{-32}	-1.61317×10^{-32}

Using these cooling rates, Melin et al.[58] were able to demonstrate that cooling by H_3^+ could more or less offset the heating in Jupiter's auroral/polar atmosphere due to the influx of energetic particles but was not able to do so for Saturn.[67] Koskinen et al.[52] also demonstrated that the H_3^+ thermostat—the trade-off between ionization due to stellar EUV and subsequent H_3^+ cooling, on the one hand, and stellar radiation heating the atmosphere, on the other—was able to stabilize a Jupiter-like planet as close as 22 × 10^6 km from a sun-like star, before its atmosphere started to undergo hydrodynamic escape.

Given its importance in governing conditions in (exo)-planetary upper atmospheres, we have now recalculated the $E(H_3^+,T)$ curve, but making use of the full transition set of

dx.doi.org/10.1021/jp312468b | J. Phys. Chem. A 2013, 117, 9770−9777

NMT and the new partition functions given in Miller et al.[59] Our calculations initially make use of $z(T)$ given in Table 1. One problem with this cooling function is that it makes use of NT's most complete partition function, which includes energy levels extrapolated via the Padé approximants up to $J = 46$ and $E_{level} = 35\,000$ cm^{-1}. However, transitions are only available for levels with J up to 20 and $E_{level} = 15\,000$ cm^{-1}. So the total emission that is being calculated is effectively too low, because transitions between energy levels from $J = 20$ to $J = 46$ and between $E_{level} = 15\,000$ and 35 000 cm^{-1} are not included in the calculation of $E(H_3^+,T)$, even though the energy levels do go into the calculation of $z(T)$.

To allow for the missing transitions, therefore, we have scaled the value of $E(H_3^+,T)$ by a factor given by

$$s_z(T) = 2.0 - z_{fp}(T)/z(T) \quad (6)$$

where $z_{fp}(T)$ is computed from the first principles levels only (Table 2). This scaling assumes the missing levels make a pro-rata contribution.

Table 4 shows that the values of $E(H_3^+,T)$ using these partition functions are identical up to 2000 K, because the partition functions are equal to that point, and that differences are within less than 2% up to 2500 K and less than 8% at 3000 K. After that, the value of $E(H_3^+,T)$ calculated with $z_{fp}(T)$ increases in comparison with that using $z(T)$ from all levels, as the latter partition function increases more rapidly with temperature: at 5000 K $E(H_3^+,T)$ calculated from $z_{fp}(T)$ is a factor of 1.4 times greater.

Table 4 also shows that our new calculation of $E(H_3^+,T)$ is greater than that derived from the Melin[67] function for all valid temperatures for which that function was derived. At 500 K, the difference is already ~35%, rising to a factor of ~2.5 at 2000 K. At temperatures above 2000 K, Melin did not claim his function was reliable, and this is clearly seen as it actually starts to decrease in value at $T > 4000$ K.

Table 4. Values for $E(H_3^+,T)$ Extrapolated for the Melin Fit Compared with Those Calculated Here in Units of Watts Molecule^{-1} Sterradian^{-1}

T (K)	$E(H_3^+,T)$ (Melin 2006)	$E(H_3^+,T)$ using $(z_{35000}(T))$	$E(H_3^+,T)$ (scaled)
500	0.50484×10^{-21}	0.67786×10^{-21}	0.67786×10^{-21}
1000	0.22120×10^{-19}	0.33393×10^{-19}	0.33393×10^{-19}
1500	0.97975×10^{-19}	0.19205×10^{-18}	0.19205×10^{-18}
2000	0.23935×10^{-18}	0.60456×10^{-18}	0.60456×10^{-18}
2500	0.43479×10^{-18}	0.12736×10^{-17}	0.12985×10^{-17}
3000	0.64867×10^{-18}	0.20089×10^{-17}	0.21598×10^{-17}
3500	0.82113×10^{-18}	0.26726×10^{-17}	0.30432×10^{-17}
4000	0.86814×10^{-18}	0.31158×10^{-17}	0.38133×10^{-17}
4500	0.68146×10^{-18}	0.33158×10^{-17}	0.43750×10^{-17}
5000	0.12867×10^{-18}	0.34119×10^{-17}	0.47688×10^{-17}

On the basis of these new calculations, we have parametrized the cooling curves. This time, our fit is to the following form:

$$\log_e\{E(H_3^+,T)\} = \sum_n C_n T^n \quad (7)$$

and covering a wide temperature range, from 30 to 5000 K. Varying degrees of fit were required, depending on the temperature range. Our best fits to the curve calculated using $z(T)$ are given in Table 5. We have also fitted the scaled cooling function to the same function for the region $T = 1800-5000$ K, where $z_{fp}(T)$ is less than $z(T)$ due to the exclusion of extrapolated levels. Our best fit values are given, with errors over the entire range of less than 0.1%, in Table 5 (last column).

Figure 1 shows the values of $\log_e\{E(H_3^+,T)\}$ and the percentage error in the actual value of $E(H_3^+,T)$ itself against temperature for the cooling curve based on the emission from the first principles calculated states and using $z(T)$. The largest errors in the fitted values of $E(H_3^+,T)$ occur for the lowest temperature range, for which they are between a maximum of ±5%. For the 30−300 K range, we use the "brute force" values of $z(T)$ rather than a fit.

Between 300 and 800 K, the errors in $E(H_3^+,T)$ are generally less than 0.1%, except at the lower end and are all but nonexistent for the 800−1800 K range. From 1800 to 5000 K, the errors increase again to a few tenths of a percent. These ranges are the most important for H_3^+ cooling, covering the full range of temperatures found in planetary atmospheres up to a point where H_3^+ and, even more importantly, its feedstock H_2 are subject to considerable thermal dissociation. Above 5000 K, our calculation of $E(H_3^+,T)$ almost certainly misses higher energy transitions, and the errors on the fit creep back toward ±0.5%. We do not report these values here.

Given the absence of calculated transitions between missing higher energy states, discussed above, it is clear there is additional uncertainty in the values of $E(H_3^+,T)$. At this stage, however, any attempt at quantification of this uncertainty would be speculation, and our $s_z(T)$ parameter must be viewed as generating an effective cooling curve. New calculations of H_3^+ energy levels and linelists would be welcome if further progress is to be made.

Table 5. Fit Coefficients for the Cooling Function $\log_e\{E(H_3^+,T)\} = \Sigma_n C_n T^n$ Using $z(T)$ and $z_{fp}(T)$ in Units of Watts Molecule^{-1} Sterradian^{-1}

range	30−300 K	300−800 K	800−1800 K	1800−5000 K using $z(t)$	1800−5000 K using $z_{fp}(T)$
C_0	−81.9599	−92.2048	−62.7016	−55.7672	−51.8647
C_1	+0.886768	+0.298920	+0.0526104	+0.0162530	+0.0101713
C_2	−0.0264611	−0.000962580	-7.22431×10^{-05}	-7.68583×10^{-06}	-4.02390×10^{-06}
C_3	+0.000462693	$+1.82712 \times 10^{-06}$	$+5.93118 \times 10^{-08}$	$+1.98412 \times 10^{-09}$	$+9.08596 \times 10^{-10}$
C_4	-4.70108×10^{-06}	-2.04420×10^{-09}	-2.83755×10^{-11}	-2.68044×10^{-13}	-1.11431×10^{-13}
C_5	$+2.84979 \times 10^{-08}$	$+1.24970 \times 10^{-12}$	$+7.35415 \times 10^{-15}$	$+1.47026 \times 10^{-17}$	$+5.69298 \times 10^{-18}$
C_6	-1.03090×10^{-10}	-3.22212×10^{-16}	-8.01994×10^{-19}		
C_7	$+2.13794 \times 10^{-13}$				
C_8	-2.26029×10^{-16}				
C_9	$+8.66357 \times 10^{-20}$				

dx.doi.org/10.1021/jp312468b | J. Phys. Chem. A 2013, 117, 9770−9777

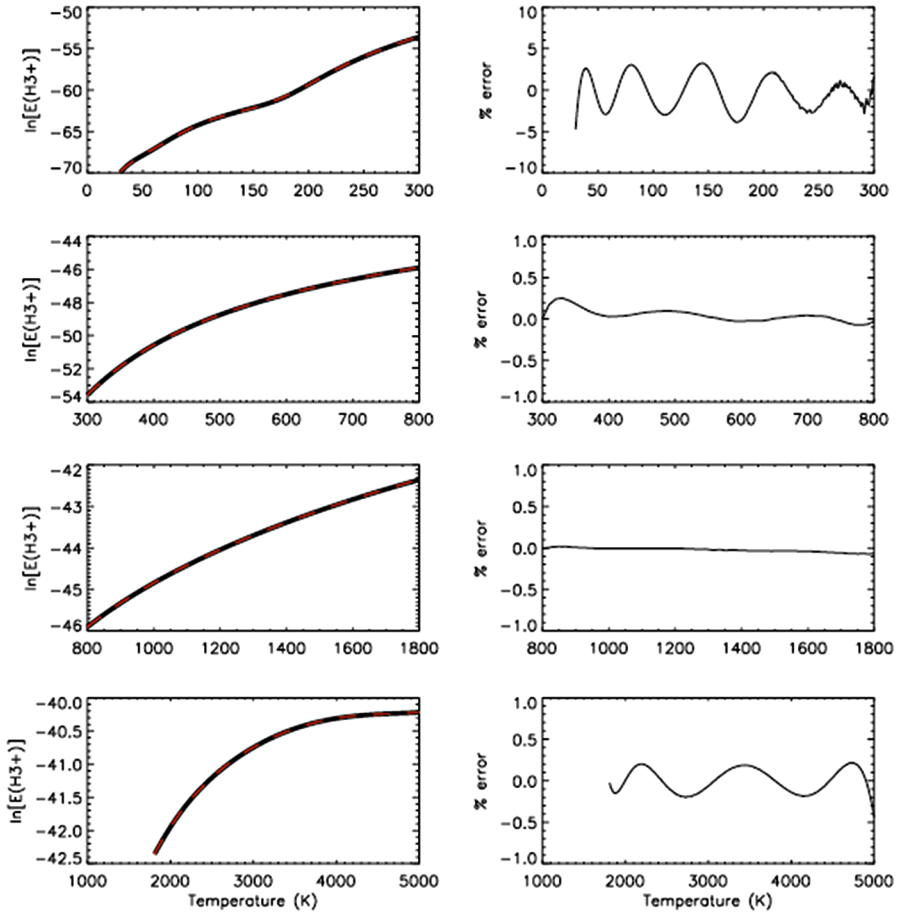

Figure 1. Left column: $\log_e\{E(H_3^+,T)\}$ vs T. Right column: percent error in $E(H_3^+,T)$ vs T. The values given here make use of $z_{35000}(T)$. The units of $E(H_3^+,T)$ are Watts molecule^{-1} sterradian^{-1}.

NON-LTE EFFECTS

Planetary upper atmospheres typically span the density range $10^{12}-10^{20}$ m^{-3} from the exosphere down to the homopause,[36,37] so H_2 energy levels are generally populated according to an LTE distribution there (see, e.g., Coppola et al.[68] and references therein). But the high values of A_{if} for H_3^+ mean that radiative relaxation is competitive with collisional deexcitation at much higher densities, probably up to $10^{17}-10^{18}$ m^{-3}, dependent on temperature. This means that H_3^+ levels are often subthermally populated for much of the gas column. Miller et al.[41] referred to the levels as being quasi-thermally populated in these regions, by which they meant

(a) that, although the level populations were generally subthermal with respect to the ground state, ratios of emitting vibrationally excited level populations were close to what would be expected from LTE and
(b) that, because H_3^+ had no permanent dipole, rotational sublevels within any particular vibrational manifold were generally populated in the same ratio as would be expected from LTE.

This means it has been possible to use H_3^+ line ratios to derived column temperatures (and effective column densities) to characterize the upper atmospheres of the giant planets, to study energy deposition and generation and changes due to solar wind−magnetosphere−ionosphere coupling processes.[54−56]

With the development of (global circulation) models capable of including the effects of H_3^+ production either by explicit means[48,69] or in a parametrized fashion,[49−52,70] it has become important to model the H_3^+ emission by taking account the line production along the line-of-sight, i.e., throughout the column of the atmosphere. In turn, this means allowing for the departure from LTE as a function of altitude/local density and local temperature to model correctly the energy balance in the atmosphere and to compare with measured H_3^+ emission.[50−52,70]

Oka and Epp[71] have developed a very elegant formulation of the detailed balance calculations required to allow for non-LTE effects for H_3^+ in a predominantly H_2 atmosphere; their aim was to compute departures of individual *rotational* levels from thermal population, which subsequent observations confirmed.[72,73] We have adapted this approach to compute the departure from LTE of the population of individual *vibrational* levels.[59] We then use this to scale the overall emission from H_3^+ making use of Miller et al.'s[41] approximation (b), using

$$s_{\mathrm{nonLTE}}(T,[H_2]) = \sum_V N_{\mathrm{nonLTE}}(V,T,[H_2])I(V) \Big/ \sum_V N_{\mathrm{LTE}}(V,T)I(V) \quad (8)$$

where $N_{\mathrm{nonLTE}}(V,T,[H_2])$ is the population of vibrational level V that comes out of the detailed balance calculation at a temperature of T and an H_2 number density of $[H_2]$,

dx.doi.org/10.1021/jp312468b | J. Phys. Chem. A 2013, 117, 9770−9777

Table 6. H_3^+ per Molecule Emission[a] and Non-LTE Scaling Factor as a Function of T and $[H_2]$

T (K)/$[H_2]$ (m^{-3})	10^{12}	10^{14}	10^{16}	10^{18}	10^{20}
300	0.36090×10^{-25}	0.21031×10^{-23}	0.52688×10^{-23}	0.53494×10^{-23}	0.53503×10^{-23}
	0.0067	0.3931	0.9848	0.9998	1.0000
600	0.24926×10^{-23}	0.73027×10^{-22}	0.17356×10^{-20}	0.23219×10^{-20}	0.23299×10^{-20}
	0.0011	0.0313	0.7449	0.9965	1.0000
1000	0.43876×10^{-22}	0.35956×10^{-21}	0.16548×10^{-19}	0.32950×10^{-19}	0.33392×10^{-19}
	0.0013	0.0108	0.4955	0.9866	0.9999
1500	0.24890×10^{-21}	0.12329×10^{-20}	0.69923×10^{-19}	0.18637×10^{-18}	0.19205×10^{-18}
	0.0013	0.0064	0.3640	0.9701	0.9997
2000	0.67354×10^{-21}	0.29496×10^{-20}	0.17497×10^{-18}	0.57434×10^{-18}	0.60431×10^{-18}
	0.0011	0.0049	0.2894	0.9499	0.9995
2500	0.12513×10^{-20}	0.53968×10^{-20}	0.32046×10^{-18}	0.12069×10^{-17}	0.12968×10^{-17}
	0.0010	0.0042	0.2469	0.9299	0.9992
3000	0.18641×10^{-20}	0.81666×10^{-20}	0.47956×10^{-18}	0.19736×10^{-17}	0.21580×10^{-17}
	0.0009	0.0038	0.2220	0.9136	0.9990
3500	0.24196×10^{-20}	0.10847×10^{-19}	0.62835×10^{-18}	0.27436×10^{-17}	0.30401×10^{-17}
	0.0008	0.0036	0.2064	0.9014	0.9988
4000	0.28498×10^{-20}	0.13073×10^{-19}	0.74751×10^{-18}	0.34010×10^{-17}	0.38065×10^{-17}
	0.0007	0.0034	0.1961	0.8923	0.9987
4500	0.31218×10^{-20}	0.14624×10^{-19}	0.82649×10^{-18}	0.38740×10^{-17}	0.43690×10^{-17}
	0.0007	0.0033	0.1889	0.8854	0.9985
5000	0.32787×10^{-20}	0.15644×10^{-19}	0.87518×10^{-18}	0.41948×10^{-17}	0.47587×10^{-17}
	0.0007	0.0033	0.1836	0.8802	0.9985

[a]Units: Watts molecule^{-1} sterradian^{-1}.

$N_{LTE}(V,T)$ is the corresponding LTE population, and $I(V)$ is given by

$$I(V) = \sum_{V'<V} (E_V - E_{V'})A_{V,V'} \quad (9)$$

which allows for the relative brightness in each of the vibration-only transitions that depopulate level V and $A_{V,V'}$ is taken from Dinelli et al.[15] Vibrational excitation and de-excitation of H_3^+ in an H_2 atmosphere has not been studied experimentally but probably, as is the case with rotational excitation and de-excitation, proceeds most efficiently through the proton-hopping reaction:

$$H_3^+(v{=}m) + H_2 \rightarrow H_2 + H_3^+(v{=}n) \quad (10)$$

We therefore use the same rate coefficient (2×10^{-15} m^3 s^{-1}) as Oka and Epp[71] for this reaction. We note that these authors point out that this is the greatest source of uncertainty in their calculation, and it is in ours, too.

Table 6 gives sample results for our non-LTE emission calculations. (Note that these values may be upper limits, especially at low densities, because we have taken the Oka and Epp[71] rate coefficient.) They show the huge variation in $E(H_3^+)$ as a function of temperature and $[H_2]$ values typical in a planetary atmosphere. Clearly, the scaling factor, $s_{nonLTE}(T, [H_2])$, plays a major role in determining the overall emission: at the lowest densities and the highest temperatures, less than 0.1% of the LTE emission is being generated, which severely limits the ability of H_3^+ to cool the exospheres of "hot Jupiter" exoplanets.

For the exospheres of the solar system giants, where T_{exo} lies between 400−600 K (Saturn) and 1100−1500 K (Jupiter), emission levels fall off rapidly with altitude. For example, the emission at 1000 K and $[H_2] = 10^{16}$−10^{18} m^{-3}, where $[H_3^+]$ tends to have its peak, is between 1 and 2 orders of magnitude greater than for higher altitudes where $T \sim 1500$ K but $[H_2] = 10^{12}$−10^{14} m^{-3}. As a result, high altitude energy inputs due to solar EUV or (lower energy) particles will heat this region more efficiently than higher energy (1−100 keV) electrons that penetrate almost to the homopause in the auroral/polar regions.[69] But the low emission levels mean that space- or ground-based observations of H_3^+ are not very sensitive to the higher altitudes. It should also be noted that calculations of overall cooling rates from an atmospheric column may need to take into account optical depth effects, although this has been shown not to be necessary for Jupiter, even in the auroral regions.[74] It may become an issue, however, for "hot Jupiters" where H_3^+ densities can exceed those in Jupiter's auroral regions.

CONCLUSIONS

It is clear from our new fits to the H_3^+ cooling curve that previous versions of this have underestimated the role of $E(H_3^+)$ in the thermal balance of planetary atmospheres. This is less important at lower temperatures but can be as much as a factor of 2 at 1500 K, which is about the highest temperature reached in Jupiter's exosphere, and even higher at higher temperatures, such as are produced in exoplanet atmospheres. Given the other uncertainties that are explicit and implicit in current models, it is not clear how significant this will turn out to be. But as those uncertainties are gradually made more certain, it is important that the full impact of H_3^+ cooling be taken into account. These new fits should help to ensure that is possible.

A program to calculate cooling due to H_3^+, H3Pcool, is part of the Europlanet Joint Research Activity 3 and is available to run on user specified grid of temperatures and local densities at http://astroweb.projects.phys.ucl.ac.uk/europlanetjra3/h3pcool/.

AUTHOR INFORMATION

Corresponding Author

*Tel: +44 20 7779 3490. E-mail: s.miller@ucl.ac.uk.

Notes

The authors declare no competing financial interest.

■ ACKNOWLEDGMENTS

We thank Oka for his inspirational work on the H_3^+ molecule and for many years of encouragement in our efforts to work on this system. We thank two anonymous referees who have helped us to improve this paper. Much of the work reported here was carried out as part of the Europlanet Research Infrastructure project funded by the European Commission's Framework 7 Programme under Contract Number 228319.

■ REFERENCES

(1) Thomson, J. J. Rays of Positive Electricity. *Philos. Mag.* **1911**, *21*, 225−249.
(2) Thomson, J. J. Some Further Applications of the Method of Positive Rays. *Nature* **1913**, *91*, 333−337.
(3) Thomson, J. J. Rays of Positive Electricity. *Proc. R. Soc.* **1913**, *A89*, 1−20.
(4) Oka, T. Observation of the Infrared Spectrum of H_3^+. *Phys. Rev. Lett.* **1980**, *45*, 531−534.
(5) Lepp, S.; Stancil, P. C.; Dalgarno, A. Chemistry of the Early Universe. *Mem. S. A. It.* **1998**, *69*, 331−336.
(6) Lepp, S.; Stancil, P. C.; Dalgarno, A. Atomic and Molecular processes in the Early Universe. *J. Phys. B* **2002**, *35*, R57−R80.
(7) Hogness, T. R.; Lunn, E. G. The Ionisation of Hydrogen by Electron Impact as interpreted by Positive Ray Analysis. *Phys. Rev.* **1925**, *26*, 44−55.
(8) Glover, S. C. O.; Savin, D. W. Is H_3^+ Cooling Ever Important in Primordial Gas? *Mon. Not. R. Astron. Soc.* **2009**, *393*, 911−948.
(9) Wolniewicz, L.; Simbotin, I.; Dalgarno, A. Quadrupole Transition Probabilities for the Excited Rovibrational States of H_2. *Astrophys. J. Suppl. Ser.* **1998**, *115*, 293−303.
(10) Kao, L.; Oka, T.; Miller, S.; Tennyson, J. A Compendium of Astronomically Important Ro-Vibrational Transitions for the H_3^+ Molecular Ion. *Astrophys. J. Suppl. Ser.* **1991**, *77*, 317−329.
(11) Sutcliffe, B. T.; Tennyson, J. A Generalised Approach to the Calculation of Ro-Vibrational Spectra of Triatomic Molecules. *Mol. Phys.* **1986**, *58*, 1067−1085.
(12) Pan, F.-S.; Oka, T. Calculated Forbidden Rotational Spectra of H_3^+. *Astrophys. J.* **1986**, *305*, 518−525.
(13) Miller, S.; Tennyson, J. Calculated Rotational and Ro-Vibrational Transitions in the Spectrum of H_3^+. *Astrophys. J.* **1988**, *335*, 486−490.
(14) Watson, J. K. G.; Foster, S. C.; McKellar, A. R. W.; Bernath, P.; Amano, T.; Pan, F.-S.; Crofton, M. W.; Altman, R. S.; Oka, T. The Infrared Spectrum of the ν_2 Fundamental Band of the H_3^+ Molecular Ion. *Can. J. Phys.* **1984**, *62*, 1875−1885.
(15) Dinelli, B. M.; Miller, S.; Tennyson, J. Bands of H_3^+ up to $4\nu_2$: Rovibrational Transitions from First Principles. *J. Mol. Spectrosc.* **1992**, *153*, 718−725.
(16) Pavanello, M.; Adamowicz, L.; Alijah, A.; Zobov, N. F.; Mizus, I. I.; Polyansky, O. L.; Tennyson, J.; Szidarovszky, T.; Csaszar, A. G.; Berg, M.; et al. Precision Measurements and Computations of Transition Energies in Rotationally Cold Triatomic Hydrogen Ions up to the Mid-Visible Spectral Range. *Phys. Rev. Lett.* **2012**, *108*, 023002.
(17) Miller, S.; Tennyson, J. Hot Band Transitions in H_3^+: First Principles Calculations. *J. Mol. Spectrosc.* **1989**, *136*, 223−240.
(18) Bawendi, M. G.; Rehfuss, B. D.; Oka, T. Laboratory Observation of Hot Bands of H_3^+. *J. Chem. Phys.* **1990**, *93*, 6200−6209.
(19) Xu, L.-W.; Gabrys, C. M.; Oka, T. Observation of the $2\nu_2(l=2) \leftarrow 0$ Overtone of H_3^+. *J. Chem. Phys.* **1990**, *93*, 6210−6215.
(20) Lee, S. S.; Ventrudo, B. F.; Cassidy, D. T.; Oka, T.; Miller, S.; Tennyson, J. Observation of the $3\nu_2 \rightarrow 0$ Overtone Band of H_3^+. *J. Mol. Spectrosc.* **1991**, *145*, 222−224.
(21) Xu, L.-W.; Rösslein, M.; Gabrys, C. M.; Oka, T. Observation of the Infrared Forbidden Transitions of H_3^+. *J. Mol. Spectrosc.* **1992**, *153*, 726−737.
(22) Ventrudo, B. F.; Cassidy, D. T.; Guo, Z. Y.; Joo, S.; Lee, S. S.; Oka, T. Near Infrared $3\nu_2$ Overtone Band of H_3^+. *J. Chem. Phys.* **1994**, *100*, 6263−6266.
(23) Uy, D.; Gabrys, C. M.; Jagod, M.-F.; Oka, T. Spectral Lines and Distribution of H_3^+ in High Rotational Levels. *J. Chem. Phys.* **1994**, *100*, 6267−6274.
(24) McCall, B. J.; Oka, T. Combination Band Spectroscopy of H_3^+. *J. Chem. Phys.* **2000**, *113*, 3104−3110.
(25) Gottfried, J. L. Near Infrared Spectroscopy of H_3^+ above the Barrier to Linearity. *Philos. Trans. R. Soc. Lond. A* **2006**, *364*, 2917−2929.
(26) Trafton, L. M.; Miller, S.; Lacy, J. H.; Greathouse, T. K. Search for Mid-IR rotational and $\nu_1 \rightarrow \nu_2$ Difference Band H_3^+ Emission in Jupiter's Northern Aurora. *Icarus* **2009**, *203*, 189−197.
(27) Watson, W. D. The Rate of Formation of Interstellar Molecules by Ion−Molecule Reactions. *Astrophys. J.* **1973**, *183*, L17−L20.
(28) Herbst, E.; Klemperer, W. Formation and Depletion of Molecules in Dense Interstellar Clouds. *Astrophys. J.* **1973**, *185*, 505−533.
(29) Martin, D. W.; McDaniel, E. W.; Meeks, M. L. On the Possible Occurrence of H_3^+ in Interstellar Space. *Astrophys. J.* **1961**, *134*, 1012−1013.
(30) Oka, T. A Search for Interstellar H_3^+. *Philos. Trans. R. Soc. Lond. A* **1981**, *303*, 543−549.
(31) Geballe, T. R.; Oka, T. Detection of H_3^+ in Interstellar Space. *Nature* **1996**, *384*, 334−335.
(32) McCall, B. J.; Geballe, T. R.; Hinkle, K. H.; Oka, T. Observations of H_3^+ in Dense Molecular Clouds. *Astrophys. J.* **1999**, *522*, 338−348.
(33) McCall, B. J.; Geballe, T. R.; Hinkle, K. H.; Oka, T. Detection of H_3^+ in the Diffuse Interstellar Medium towards Cygnus OB2. *Science* **1998**, *279*, 1910−1913.
(34) Goto, M.; McCall, B. J.; Geballe, T. R.; Usuda, T.; Kobayashi, N.; Terada, H.; Oka, T. Absorption Line Survey of H_3^+ towards the Galactic Centre Sources I: GCS 3−2 and GC IRS3. *Publ. Astron. Soc. Jpn.* **2002**, *54*, 951−961.
(35) Geballe, T. R.; Goto, M.; Usuda, T.; Oka, T.; McCall, B. J. The Interstellar Medium of IRAS 08572 + 3915 NW: H_3^+ and Warm High-Velocity CO. *Astrophys. J.* **2006**, *644*, 907−913.
(36) Atreya, S. K.; Donahue, T. M. Ionosphere. In *Jupiter*; Gehrels, T., Ed.; University of Arizona Press: Tucson, AZ, 1976; pp 304−310.
(37) Atreya, S. K. *Atmospheres and Ionospheres of the Outer Planets*; Springer Verlag: Heidelberg, 1986.
(38) Trafton, L. M.; Carr, J.; Lester, D.; Harvey, P. Unidentified Lines in the Spectrum of Jupiter. In Time Variable Phenomena in the Jovian system; Belton, M. J. S., West, R. A., Rahe, J., Eds.; NASA: Washington, DC, 1989; pp 229−233.
(39) Drossart, P.; Maillard, J.-P.; Caldwell, J.; Kim, S. J.; Watson, J. K. G.; Majewski, W. A.; Tennyson, J.; Miller, S.; Atreya, S.; Clarke, J.; et al. Detection of H3+ on Jupiter. *Nature* **1989**, *340*, 539−541.
(40) Maillard, J.-P.; Drossart, P.; Watson, J. K. G.; Kim, S. J.; Caldwell, J. H_3^+ Fundamental Band in Jupiter's Auroral Zones at High Resolution from 2400 to 2900 Inverse Centimeters. *Astrophys. J.* **1990**, *363*, L37−L41.
(41) Miller, S.; Joseph, R. D.; Tennyson, J. Infrared Emissions of H_3^+ in the Atmosphere of Jupiter in the 2.1 and 4.0 Micron Region. J. *Astrophys. J.* **1990**, *360*, L55−L58.
(42) Oka, T.; Geballe, T. R. Observations of the 4-Micron Fundamental Band of H_3^+ in Jupiter. *Astrophys. J.* **1990**, *351*, L53−L56.
(43) Geballe, T. R.; Jagod, M.-F.; Oka, T. Detection of H_3^+ from Saturn. *Astrophys. J.* **1993**, *410*, L109−L112.
(44) Trafton, L. M.; Geballe, T. R.; Miller, S.; Tennyson, J. Detection of H_3^+ from Uranus. *Astrophys. J.* **1993**, *405*, 761−766.
(45) Stallard, T.; Miller, S.; Millward, G.; Joseph, R. D. On the Dynamics of the Jovian Ionosphere and Thermosphere I: The Measurement of Ion Winds. *Icarus* **2001**, *154*, 475−491.

(46) Raynaud, E.; Lellouch, E.; Maillard, J.-P.; Gladstone, G. R.; Waite, J. H., Jr.; Bézard, B.; Drossart, P.; Fouchet, T. Spectro-Imaging Observations of Jupiter's 2-μm Auroral Emission. I. H_3^+ Distribution and Temperature. *Icarus* **2004**, *171*, 133−152.
(47) Melin, H.; Stallard, T.; Miller, S.; Lystrup, M. B.; Trafton, L. M.; Booth, T. C.; Rivers, C. New Limits on H_3^+ Abundance on Neptune Using Keck NIRSPEC. *Mon. Not. R. Astron. Soc.* **2011**, *410*, 641−644.
(48) Achilleos, N.; Miller, S.; Tennyson, J.; Aylward, A. D.; Mueller-Wodarg, I.; Rees, D. JIM: A Time-Dependent, Three-Dimensional Model of Jupiter's Thermosphere and Ionosphere. *J. Geophys. Res.* **1998**, *103*, 20 089−20112.
(49) Bougher, S. W.; Waite, J. H.; Majeed, T.; Gladstone, G. R. Jupiter Thermospheric General Circulation Model (JTGCM): Global structure and Dynamics driven by Auroral and Joule Heating. *J. Geophys. Res.* **2005**, DOI: 10.1029/2003JE002230.
(50) Smith, C. G. A.; Aylward, A. D.; Miller, S.; Müller-Wodarg, I. C. F. Polar Heating in Saturn's Thermosphere. *Ann. Geophys.* **2005**, *23*, 2465−2477.
(51) Müller-Wodarg, I. C. F.; Moore, L.; Galand, M.; Miller, S.; Mendillo, M. Magnetosphere-Atmosphere Coupling at Saturn: 1 - Response of Thermosphere and Ionosphere to Steady State Polar Forcing. *Icarus* **2012**, *221*, 481−494.
(52) Koskinen, T. T.; Aylward, A. D.; Miller, S. A Stability Limit for Giant Exoplanet Atmospheres. *Nature* **2007**, *450*, 845−848.
(53) Connerney, J. E. P.; Satoh, T. The H_3^+ Ion: a Remote Diagnostic of the Jovian Magnetosphere. *Philos. Trans. R. Soc. Lond. A* **2000**, *358*, 2471−2483.
(54) Lellouch, E. Spectro-imaging Observations of H_3^+ on Jupiter. *Philos. Trans. R. Soc. Lond. A* **2006**, *364*, 3139−3146.
(55) Miller, S.; Achilleos, N.; Ballester, G. E.; Geballe, T. R.; Joseph, R. D.; Prange, R.; Rego, D.; Stallard, T.; Tennyson, J.; Trafton, L. M.; Waite, J. H. The role of H_3^+ in Planetary Atmospheres. *Philos. Trans. R. Soc. Lond. Trans. A* **2000**, *358*, 2485−2502.
(56) Miller, S.; Stallard, T.; Smith, C. H_3^+: The Driver of Planetary Atmospheres. *Philos. Trans. R. Soc. Lond. Trans. A* **2006**, *364*, 3121−3137.
(57) Stallard, T. S.; Melin, H.; Miller, S.; O'Donoghue, J.; Cowley, S. W. H.; Badman, S. V.; Adriani, A.; Brown, R. H.; Baines, K. H. Temperature Changes and Energy Inputs in Giant Planet Atmospheres: what We are Learning from H_3^+. *Philos. Trans. R. Soc. Lond. A* **2012**, *370*, 5213−5224.
(58) Melin, H.; Miller, S.; Stallard, T.; Smith, C.; Grodent, D. Energy Balance in the Jovian Atmosphere during an Auroral Heating Event. *Icarus* **2006**, *181*, 256−265.
(59) Miller, S.; Stallard, T.; Melin, H.; Tennyson, J. H_3^+ Cooling in Planetary Atmospheres. *Faraday Discuss.* **2010**, *147*, 283−291.
(60) Koskinen, T. T.; Aylward, A. D.; Miller, S. The Upper Atmosphere of HD171561b. *Astrophys. J.* **2009**, *693*, 868−885.
(61) Chandra, S.; Gaur, V. P.; Pande, M. C. The Partition Function of H_3^+. *J. Quantum Spectrosc. Radiat. Transf.* **1991**, *45*, 57−61.
(62) Sidhu, K. S.; Miller, S.; Tennyson, J. Partition Functions and Equilibrium Constants for H_3^+ and H_2D^+. *Astron. Astrophys.* **1992**, *255*, 453−456.
(63) Neale, L.; Tennyson, J. A High Temperature Partition Function for H_3^+. *Astrophys. J.* **1995**, *454*, L169−L173.
(64) Bergeron, P.; Ruiz, M. T.; Leggett, S. K. The Chemical Evolution of Cool White Dwarfs and the Age of the Local Galactic Disk. *Astrophys. J. Suppl. Ser.* **1997**, *108*, 339−387.
(65) Neale, L.; Miller, S.; Tennyson, J. Spectroscopic Properties of the H_3^+ Molecule: A New Calculated Line List. *Astrophys. J.* **1996**, *464*, 516−520.
(66) Melin, H. Comparative Aeronomy of the Upper Atmospheres of the Giant Planets. *Ph.D. Thesis*, University College London, 2006
(67) Melin, H.; Miller, S.; Stallard, T.; Trafton, L. M.; Geballe, T. R. Variability in the H_3^+ Emission from Saturn: Consequences for Ionisation Rates and Temperature. *Icarus* **2007**, *186*, 234−241.
(68) Coppola, C. M.; D'Introno, R.; Galli, D.; Tennyson, J.; Longo, S. Non-equilibrium H_2 Formation in the Early Universe: Energy Exchanges, Rate Coefficients and Spectral Distortions. *Astrophys. J. Suppl. Ser.* **2012**, *199*, 16−22.
(69) Grodent, D.; Waite, J. H., Jr.; Gerard, J.-C. A Self-consistent Model of the Jovian Auroral Thermal Structure. *J. Geophys. Res.* **2001**, *106*, 12933−12952.
(70) Galand, M.; Moore, L.; Müller-Wodarg, I. C. F.; Mendillo, M.; Miller, S. Response of Saturn's Auroral Ionosphere to Electron Precipitation: Electron Density, Electron Temperature and Electrical Conductivity. *J. Geophys. Res.* **2011**, *116*, A09306.
(71) Oka, T.; Epp, E. Non-thermal Rotational Distribution of H_3^+. *Astrophys. J.* **2004**, *613*, 349−354.
(72) Oka, T.; Geballe, T. R.; Goto, M.; Usuda, T.; McCall, B. J. Hot and Diffuse Clouds near the Galactic Centre probed by Metastable H_3^+. *Astrophys. J.* **2005**, *632*, 882−893.
(73) Kreckel, H.; Krohn, S.; Lammich, L.; Lange, M.; Levi, J.; Scheffel, M.; Schwalm, D.; Tennyson, J.; Vager, Z.; Wester, R.; et al. Vibrational and Rotational cooling of H_3^+. *Phys. Rev. A* **2002**, *66*, 052509.
(74) Lam, H. A.; Achilleos, N.; Miller, S.; Tennyson, J.; Trafton, L. M.; Geballe, T. R.; Ballester, G. E. A Baseline Spectroscopic Study of the Infrared Aurorae of Jupiter. *Icarus* **1997**, *127*, 379−393.